Separation Science and Technology
Publication details, including instructions for authors and subscription information:
http://www.informaworld.com/smpp/title~content=t713708471

Analysis of Filtration Characteristics for Compressible Polycrystalline Particles by Partial Least Squares Regression

Ralf Beck[a]; Ketil Svinning[b]; Antti Häkkinen[c]; Didrik Malthe-Sørenssen[a]; Jens-Petter Andreassen[a]
[a] Department of Chemical Engineering, Norwegian University of Science and Technology (NTNU), Trondheim, Norway [b] POSTEC, Tel-Tek, Porsgrunn, Norway [c] Department of Chemical Technology, Lappeenranta University of Technology (LUT), Lappeenranta, Finland

Online publication date: 02 June 2010

To cite this Article Beck, Ralf , Svinning, Ketil , Häkkinen, Antti , Malthe-Sørenssen, Didrik and Andreassen, Jens-Petter(2010) 'Analysis of Filtration Characteristics for Compressible Polycrystalline Particles by Partial Least Squares Regression', Separation Science and Technology, 45: 9, 1196 — 1208
To link to this Article: DOI: 10.1080/01496391003705649
URL: http://dx.doi.org/10.1080/01496391003705649

Separation Science and Technology, 45: 1196–1208, 2010

ISSN: 0149-6395 print/1520-5754 online
DOI: 10.1080/01496391003705649

Taylor & Francis
Taylor & Francis Group

Analysis of Filtration Characteristics for Compressible Polycrystalline Particles by Partial Least Squares Regression

Ralf Beck,[1] Ketil Svinning,[2] Antti Häkkinen,[3] Didrik Malthe-Sørenssen,[1] and Jens-Petter Andreassen[1]

[1]*Department of Chemical Engineering, Norwegian University of Science and Technology (NTNU), Trondheim, Norway*
[2]*POSTEC, Tel-Tek, Porsgrunn, Norway*
[3]*Department of Chemical Technology, Lappeenranta University of Technology (LUT), Lappeenranta, Finland*

Crystal size and morphology have been varied by changing the initial supersaturation ratio and the temperature in reactive crystallization experiments. The influence of the chord length distribution, average cake porosity, and filtration pressure difference on the average cake resistance of polycrystalline particles of an industrially produced aromatic amine has been investigated by means of partial least squares (PLS) regression and sensitivity analysis. Analysis of the results has disclosed that wider chord length distributions as well as lower values of the measured average porosity lead to higher values for the average cake resistance. However, PLS regression and sensitivity analysis have identified the applied pressure difference itself as the most significant parameter influencing the magnitude of the cake resistance. This unexpected behavior is accounted for by compression of the filter cake occurring predominantly in small layers above the filter cloth characteristic for highly compressible cakes.

Keywords constant pressure cake filtration; crystallization; FBRM chord length distribution; partial least squares regression; sensitivity analysis

INTRODUCTION

Filtration of crystalline material, as well as crystal handling in other down-stream processes like washing, drying, powder transport, and powder storage is influenced by characteristic properties displayed by the crystals. Crystal properties like morphology, size, surface structure, and hardness are controlled by crystallization parameters such as the type of substance used, supersaturation (chemical potential), temperature, mixing, crystallization time, pH, solvent composition, and type and amount of seed crystals. The crystallization conditions influence the nucleation, growth, aggregation and the breakage of the crystals (1).

Received 25 November 2009; accepted 12 February 2010.
Address correspondence to Ralf Beck, Department of Chemical Engineering, NTNU, Trondheim 7491, Norway. E-mail: ralfb@chemeng.ntnu.no

Variation in the crystal properties by the applied crystallization conditions will affect the subsequent filtration process (2), which can be characterized by the specific average cake resistance. The ideal filtration theory assumes the feed suspension to consist of a constant concentration of spherical particles of the same size. The cake is assumed to build up without rearrangement and breakage of the particles in the cake and the supposed laminar filtrate flow is proportional to the cake build-up. In practice, however, suspensions are composed of non-spherical particles exhibiting a variation in size and shape. This has led to concepts that are based on the Sauter mean diameter of the distribution of particles with shape factors correcting for the deviation from spherical shapes (3,4). The filtration cake resistance is lower for larger particles (lower specific surface area) as well as for cakes exhibiting higher porosity (5). The relation between the filter cake resistance and the size is derived by Carman (6–8) from Kozeny's work (9). Leave aside the size distribution of particles, real filtration processes are also deviating from ideal conditions in other aspects. Filter cakes are usually compressible, at least to some extent, resulting in the interdependence between the applied pressure difference, porosity and cake resistance (10,11). In literature, other parameters than the applied pressure are reported to influence the cake resistance. For example, Rushton et al. (12) found that both the flow velocity and the solids concentration affect the measured cake resistance values. Cake structures were observed to be more open in experiments performed at higher velocities leading to lower average cake resistance values. Above a certain limit, the cake was also found to be more open structured at higher levels of solids concentration. As a result of the numerous parameters influencing the cake resistance, Häkkinen et al. (13) use multilinear partial least squares regression (N-PLS) as a tool to predict average specific cake resistance values, cake porosity, and cake

compressibility of sulfathiazole crystal suspensions. The model is based on shape and size data obtained from image analyser measurements as well as on the density and the viscosity of the solvents used. Multivariate data analysis has been proved to be a successful tool in various areas like research and development, process optimization and control, quality control and market research. As an example, Liotta and Sabesan (14) use the method of partial least squares (PLS) regression to predict solute concentration values of an active pharmaceutical ingredient based on infrared (ATR, attenuated total reflectance) spectra to be able to control the supersaturation level and thereby the crystal size throughout the crystallization experiment. PLS regression allows for the prediction of dependent variables based on latent variables calculated from a large number of variables as compared to observations, thus allowing for data compression (15). In PLS regression a number of factors are calculated and optimized for maximum explanation of the variance in the y-variables. The concentration (dependent variable) can be calculated from the large number of absorbance values associated to certain wave lengths of the used IR radiation (14). Togkalidou et al. (16) have previously studied different multivariate methods like partial least squares regression, principal component regression, top-down regression, and confidence interval regression to relate the chord length distributions of crystal suspensions measured by focused beam reflectance measurements (FBRM) to the measured average cake resistance values. Sensitivity analysis is concerned with how the results of estimations from PLS depend on the data set. There are two approaches to sensitivity analysis, one is to consider the influence of the samples and the other concerns the influence of the variables (17). The latter approach is applied in the present work.

Polycrystalline particles with a roughly spherical shape have been identified in the industrial production of an aromatic amine derivative, where filtration is considered to be the major bottle neck. We have previously shown that these particles are produced by a spherulitic growth mechanism (18). In the present work variations in chord length distributions obtained by FBRM (19), porosity and applied filtration pressure difference were evaluated for their effect on the average cake resistance by means of partial least squares regression and sensitivity analysis, in order to shed light on the filtration problems encountered in the industrial production of aromatic amine spherulites.

EXPERIMENTAL

Crystallization Experiments

The initial supersaturation ratio S and temperature T were varied in reactive crystallization experiments performed in a 2 l batch (18) reactor at 500 rpm stirring speed within 2 hours crystallization time after nucleation to produce crystals of different size and morphology. The initial supersaturation ratio S, was calculated as the ratio of the weight fraction of dissolved substance before the onset of nucleation to the solubility weight fraction c^*:

$$S = \frac{c}{c^*} \tag{1}$$

The initial supersaturation ratio was varied in the range from $S = 2$ to $S = 8$ and experiments were performed between 5°C and 60°C.

Non-weighted chord length distributions were recorded at the end of each experiment by means of FBRM (Mettler Toledo, Lasentec D600 L) operated in the fine resolution mode at a scanning speed of 2 m/s. The data were collected in the fine resolution mode to capture the small particles which might be of crucial importance for the filtration performance (2,20). The crystal morphology was studied by scanning electron microscopy (SEM, HITACHI, S-3400 N).

Filtration Experiments

Prior to the filtration experiments, the solids density ρ_s of the crystals was measured using a gas pycnometer (Micromeretics, AccuPyc 1330). The Dynamic viscosity η was determined by a capillary viscosimeter (Ubbelohde-viscometer, Schott Instruments, 50103 0c). The 1 liter thermostated pressure Nutsche filter with $A = 20\,\text{cm}^2$ filter area (pocket leaf filter, BHS, TMG 400) was filled with 350 ml suspension in each experiment. Polypropylene filters (Tamfelt, PP 2101) were used as filter media. Filtrate volume V, and filtration time t, were recorded by a data collection program for batch filtration experiments performed at constant pressure differences Δp of 2, 4, and 6 bar. Altogether 49 filtration experiments were performed. The effective solids concentration x_{esc} was calculated according to

$$x_{esc} = \frac{\rho_l}{\frac{1}{s_{mfs}} - \left(1 + \frac{\rho_l}{\rho_s}\frac{\varepsilon}{(1-\varepsilon)}\right)} \tag{2}$$

where ρ_l and ρ_s stand for the density of the liquid or the solid, respectively and s_{mfs} represents the mass fraction of solids in the feed. For better comparability of different filtration experiments (21,13) the solids suspension concentration was kept constant at approximately $s_{mfs} = 0.09$ by removing clear filtrate. The average cake porosity ε was calculated by Eq. (3):

$$\varepsilon = \frac{Ah - \frac{m_S}{\rho_s}}{Ah} \tag{3}$$

The cake height h as well as the mass of the dry solids m_s were measured after the filtration process. The

average specific cake resistance α was calculated from Eq. (4):

$$\frac{t}{V} = \alpha \frac{\eta x_{ecs}}{2A^2 \Delta p} V + \frac{\eta \beta}{A \Delta p} \quad (4)$$

where η is the dynamic viscosity, Δp is the applied pressure difference and β is the filter medium resistance.

Partial Least Squares Regression

PLS is performed on y-variables, expressed as a vector. The models which relate the PLS model terms are given by the following expressions:

$$\mathrm{X} = \mathrm{TP}^T + \mathrm{E} \quad (5)$$

$$\mathrm{Y} = \mathrm{UQ}^T + \mathrm{F} \quad (6)$$

T and U are factor scores, P and Q are the loadings of the x and y-variables and E and F are the residuals in X and Y, respectively. Alternatively, Eq. (5) can be expressed in the form:

$$\mathrm{X} = \mathrm{t}_1 \mathrm{p}_1^T + \mathrm{t}_2 \mathrm{p}_2^T + \cdots + \mathrm{t}_a \mathrm{p}_a^T + \cdots + \mathrm{t}_A \mathrm{p}_A^T + \mathrm{E} \quad (7)$$

where $a = A$ is equal to the maximum number of latent variables included in the PLS-model for explanation of variance in Y.

By scaling the variables, an unreasonable influence of variables with dominating standard deviations, $s(x)$, on the model can be avoided. The weighting (w) of $x_{i,k}$ by centering and scaling is performed according to the following formula, where i is the observation number and k is the number of the original variable:

$$x_{ik,w} = \frac{x_{ik} - \bar{x}_k}{s(x_k)} \quad (8)$$

Recorded chord length distributions (1–1000 μm) were divided into 45 log channels and the 7 channels with the highest chord length values were left out due to statistical insignificance. Thus, the percentage of chords between 1 μm and 317 μm from 38 channels, the pressure difference and the measured average cake porosity were chosen as independent variables x to perform PLS-regression to explain the effect on the y-variables, the measured average specific cake resistance values, α or $\log(\alpha)$. All 49 performed filtration experiments were included into the model as one sample set, giving a matrix composed of 40 x-variables (columns) and 49 samples (rows). The commercial software Unscrambler (CAMO, version 9.7) was used to perform the PLS-regression analysis. The observation X-matrix consists of observation of the following groups of variables or sub matrices: $\left(\mathrm{x}_{\Delta \mathrm{p}} | \mathrm{X}_{\text{chord length distr}} | \mathrm{x}_{\varepsilon}\right)$.

Validation

Validation means to determine the number of PLS-components or latent variables that give the prediction of y from X in future objects that lack the value of the y-variable. Cross validation was performed in this work. The calibration set was split into ten segments, and the validation was repeated ten times, each time treating one-tenth of the calibration set as prediction objects. The cross-validated residual variance in y after inclusion of A latent variables is as follows:

$$\mathrm{Var}(y)_{\mathrm{val},n} = \frac{1}{I_{pr}} \sum_{i=1}^{I_{pr}} (\hat{y}_i - y_i)^2 \quad (9)$$

where I_{pr} is equal to the number of validation objects, which is equal to the number of calibration objects, $\hat{y}_i$ is the predicted value and y_i the respective observed value.

Sensitivity Analysis

Sensitivity analysis was used to evaluate the influence of the chord length distribution data, the applied pressure difference and the porosity on the cake resistance.

Sensitivity analysis based on a PLS model performed with centered and scaled data allows for the evaluation of how the x-variables affect the chosen y-variables in different ways:

1. Comparison of the regression coefficients of the various variables from PLS with centered and scaled data.
2. Significance testing on the coefficients by application of Jack-knifing estimation (22).
3. Prediction of variation in y from variation of one x-variable in equal steps in one direction while the others are kept constant and equal to their respective mean values.

An influence of one or several x-variables on a y-variable is defined in this work as being significant if there is no overlap of confidence intervals of the predicted maximum and minimum y-values. The significance of the influence of a variable x_k is evaluated by Jackknifing estimation. This influence is defined significant if the uncertainty level is less than $2|b_{wk}|$, where b_{wk} is the regression coefficient.

The type of sensitivity analysis to be applied for examining the influence of x on y depends much on the type of modeling applied. In multivariate data analysis as for example PLS y is correlated to the latent variables which are linear combinations of the x-variables. In (23) and (24) variation in y is predicted from a simulated variation of a latent variable. The latent variable may be a combination of several.

From the PLS-model on centered and scaled data the influence of x-variables on the y-variable(s) is evaluated

by prediction of variation in y from variation of one latent variable at a time from one "observed" extreme to the other. By varying the A'th latent variable $\Delta t\,\mathrm{p}_a$ the variation in Δx_k in its original form, i.e., not scaled, can be calculated in the following way:

$$\Delta x_k = (\Delta t\, p_{ka})\, s(x_k) \tag{10}$$

Similar to a type of sensitivity analysis with variation of only one x-variable, the score, t, is varied in one direction and in equal steps, Δt. Calculation of x_k, neither centered nor scaled, will then be as follows:

$$x_k = (t\, p_{ka}) s(x_k) + \bar{x}_k \tag{11}$$

Usually, variation in the whole observation X-matrix was simulated prior to the prediction by constructing an artificial observation X-matrices. In some cases sensitivity analysis in the form of prediction from a simulated variation of a selection or a group of variables could be appropriate.

Optimization

The optimization based on the PLS-model is in the form of a linear program, where the constraints describing the influence of one variable on the others are given by one original PLS component or one equal a combination of several (25,26). Having a model $y = b_0 + \sum_{k=1}^{K} b_k x_k$ from PLS on mean-centered and scaled data, using weights based on the standard deviation and selecting the latent variable no. a to constrain the variation in X then mathematically, the linear programming problem is presented as follows:

Minimize or Maximize

$$y = \sum_{k=1}^{K} b_k x_k \quad \text{or} \quad y = \mathrm{x}^{\mathrm{T}}\mathrm{b} \tag{12}$$

subject to

$$\mathrm{A}_1\mathrm{x} = \mathrm{c}_1, \quad \mathrm{A}_2\mathrm{x} \le \mathrm{c}_2, \quad \mathrm{A}_2\mathrm{x} \ge \mathrm{c}_3 \quad \text{and} \quad \mathrm{x} \ge 0$$

where

$$\mathrm{A}_1 = \begin{pmatrix} -p_{ka}s(x_k) & \cdots & 0 & p_{1a}s(x_1) & 0 & \ldots & 0 \\ \vdots & \ddots & \vdots & \vdots & \vdots & \ddots & \vdots \\ 0 & \ldots & -p_{ka}s(x_k) & p_{k-1a}s(x_{k-1}) & 0 & \ldots & 0 \\ 0 & \ldots & 0 & p_{k+1a}s(x_{k+1}) & -p_{ka}s(x_k) & \ldots & 0 \\ \vdots & \ddots & \vdots & \vdots & \vdots & \ddots & \vdots \\ 0 & \cdots & 0 & p_{Ka}s(x_K) & 0 & \ldots & -p_{ka}s(x_k) \end{pmatrix}$$

$$\mathrm{A}_2 = \begin{pmatrix} 1 & \cdots & 0 \\ \vdots & \ddots & \vdots \\ 0 & \cdots & 1 \end{pmatrix}$$

$$\mathrm{c}_1 = \begin{pmatrix} \bar{x}_k\ p_{1a}\, s(x_1) - \bar{x}_1\ p_{ka}\, s(x_k) \\ \vdots \\ \bar{x}_k\ p_{k-1a}\, s(x_{k-1}) - \bar{x}_{k-1}\ p_{ka}\, s(x_k) \\ \bar{x}_k\ p_{k+1a}\, s(x_{k+1}) - \bar{x}_{k+1}\ p_{ka}\, s(x_k) \\ \vdots \\ \bar{x}_k\ p_{Ka}\, s(x_K) - \bar{x}_K\ p_{ka}\, s(x_k) \end{pmatrix}$$

$$\mathrm{c}_2 = \begin{pmatrix} x_{1\ upper\ \mathrm{lim}\ it} \\ \vdots \\ x_{K\ upper\ \mathrm{lim}\ it} \end{pmatrix}$$

$$\mathrm{c}_3 = \begin{pmatrix} x_{1\ lower\ \mathrm{lim}\ it} \\ \vdots \\ x_{K\ lower\ \mathrm{lim}\ it} \end{pmatrix}$$

$\bar{x}_k$, $s(x_k)$, and p_{ka} are the mean value, standard deviation, and the loading of x_k, respectively. The constant b_0 is not included in the optimization but is added afterwards. x_k is selected to influence the other x-variables in the constraints if $|p_{ka}s(x_k)|$ is of max value for $k = 1, 2, \ldots, K$.

In order to achieve the most optimal solution, several PLS-components were involved in optimization. The "loadings" in the new constraints are linear combinations of the original ones and are expressed as follows:

$$\mathrm{p}_{\text{combination of several PLS-components}} = \sum_{a=1}^{A} n_a \mathrm{p}_a \tag{13}$$

where $\sum_{a=1}^{A} n_a = 1$ and $0 < n_a < 1$.

The latter constraint prevents absolute values of the scores, $|\mathrm{t}|$, of optimal $\mathrm{x} = (x_1\ x_2 \ldots x_K)$ to be unreasonable high.

The stepwise optimization was in this case carried out, by stepwise changes of some or all $n_1, \ldots, n_A$ before the next optimization, until a maximum value of y was obtained, on the condition that the constraints were consistent.

A useful method for optimizing a combination of several latent variables is the simplex method (27). This is not to be confused with the simplex methods of linear programming.

RESULTS AND DISCUSSION

Crystal Properties and Filtration Characteristics

A limited number of the resulting crystalline products are presented to illustrate major differences in the crystal size and morphology as a consequence of different

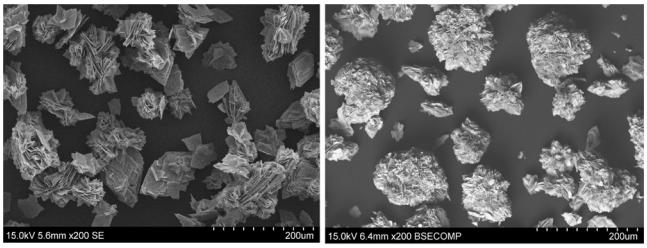

(a) (b)

FIG. 1. Crystals produced at 60°C and an initial supersaturation ratio of (a) S = 4 and (b) S = 6. The whole scale bar is 200 μm.

temperature and supersaturation in the crystallization experiments. Crystals formed at 60°C at different initial supersaturation ratios are depicted in Fig. 1, at an initial supersaturation ratio of either 4 (Fig. 1a) or 6 (Fig. 1b). At an initial supersaturation of S = 6, polycrystalline particles with a denser surface structure appear, while in experiments performed at S = 4 the crystals exhibit a more open surface structure and plate-like particles crystallize along with the polycrystalline particles. The amount of plate-like crystals was found to increase (18) in experiments performed at a lower initial supersaturation, by nucleation and growth from solution. Plate-like particles can also be formed by transformation of the polycrystalline particles or by attrition of the seemingly fragile spherulites in the course of the crystallization process. Polycrystalline particles produced at 5°C are seemingly smaller (Fig. 2b) and exhibit a more compact surface structure than spherulitic crystals originating from experiments performed at 60°C (Fig. 1b). The particles produced at 25°C (Fig. 2a) seem to be intermediate to the particles produced at 5 and 60°C, at least with respect to the maximum particle size. However, the results of the FBRM-measurements (Fig. 3) reveal a different trend for these three different crystallization conditions. SEM-pictures cannot be used to obtain information about the particle size distribution due to non-representative sampling in this case. The FBRM-measurements on the other hand, were shown to be highly reproducible. Spherulites obtained at T = 5°C and S = 8

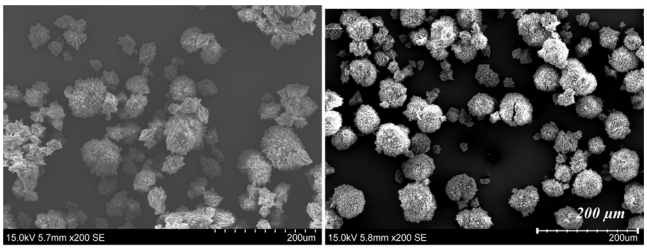

(a) (b)

FIG. 2. Crystals obtained from experiments performed at a supersaturation ratio of S = 8 at (a) 25°C and (b) 5°C.

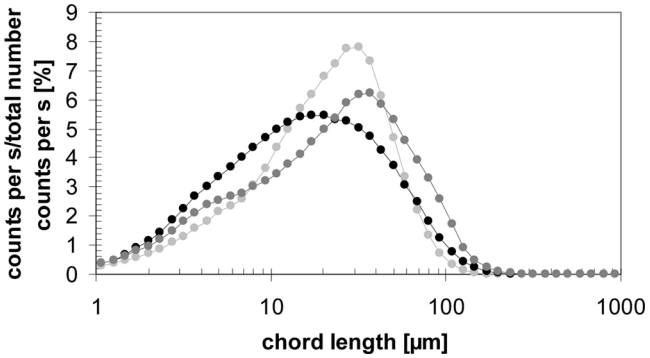

FIG. 3. Measured counts of chords per second in relation to the total number of measured counts per s divided into chord length intervals exemplified for crystals produced at T = 5°C and S = 8 (light grey), T = 25°C and S = 8 (dark grey) and T = 60°C and S = 6 (black).

(light grey spectrum in Fig. 3) exhibit a narrow chord length distribution, with the lowest frequency of counts for smaller chord lengths. Crystals (black spectrum in Fig. 3) produced at 60°C at S = 6 lead to a relatively broad chord length distribution, with a high frequency of smaller chord lengths. The distribution at 25°C and S = 8 resulted in a broad distribution with a surprisingly high frequency of larger chord lengths when compared to the particle size information from the SEM-picture of Fig. 2a.

At 2 bar filtration pressure difference, the measured average specific cake resistance value was found to be almost 9 times higher for experiments performed at 25°C and S = 8 ($2.1 \cdot 10^{10}$ m/kg) than for experiments carried out at 5°C and S = 8 ($2.4 \cdot 10^{9}$ m/kg), whereas the cake resistance was intermediate for crystal suspensions originating from experiments at 60°C and S = 6 ($7.3 \cdot 10^{9}$ m/kg).

The effect of the filtration pressure difference on the measured cake resistance values is illustrated in Fig. 4 for crystals produced at T = 60°C and S = 6. The measured cake resistance values in this figure are fitted by means of a power function.

The discrepancy in particle size observations from the SEM-pictures of Fig. 1 and 2 and the chord length

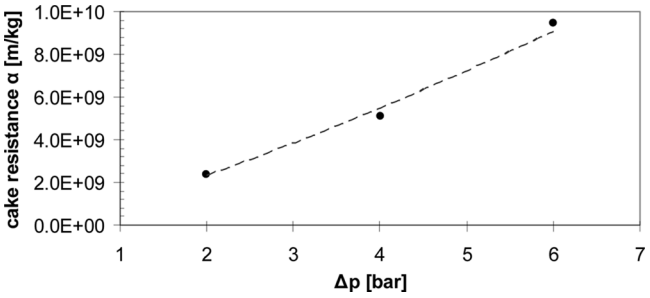

FIG. 4. The effect of the filtration pressure difference on the measured cake resistance values for the filtration of crystals produced at T = 60°C and S = 6.

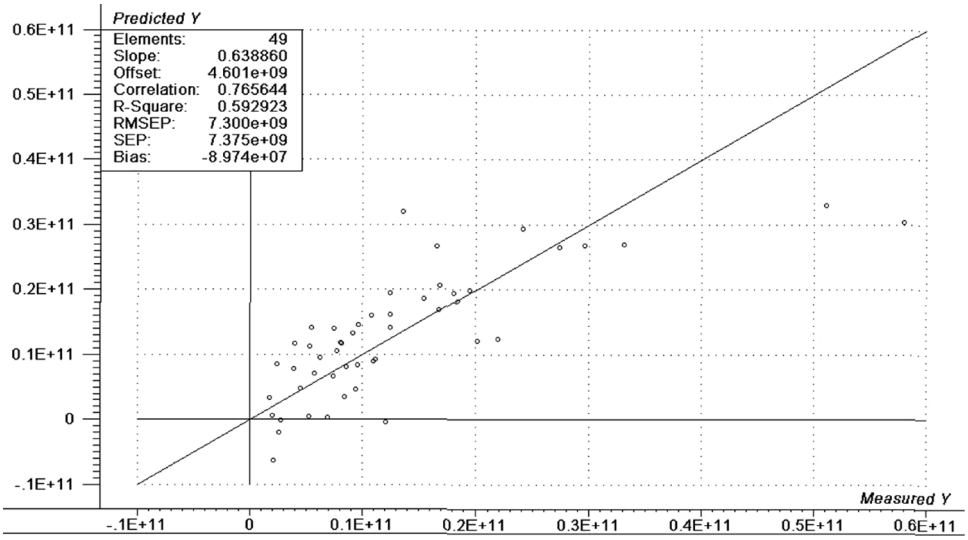

FIG. 5. Predicted versus measured values for the cake resistance α (y).

information in Fig. 3 motivated for a statistical analysis that takes the whole distribution into account. The additional large effect of pressure difference on the measured cake resistance made it obvious to include also this variable in the analysis. The average porosity was also included since it has an effect on the filter cake resistance.

Partial Least Squares Regression

PLS regression based on the 49 observations (filtration experiments) yielded maximum explained variance (59%) with 5 PLS-components incorporated into the model. The predicted values for the average specific cake resistance (α) values (predicted y) are plotted against the measured cake resistance values (measured y) in Fig. 5. The plot in Fig. 5 of predicted versus measured cake resistance shows a lack of fit appearing as systematic tendencies. Therefore another PLS model based on the logarithmic form of the cake resistance ($ln(\alpha)$) was built to examine the possibility of achieving a plot which fits the target line (predicted equal to measured values) in a better way (Fig. 6). As can be seen when comparing Figs. 5 and 6 the new model yields a better fit to the target line. The explained variance increases from 59 to 86%. However, the latter model uses 9 PLS-components, but according to Fig. 7 the increase in explained variance is marginal when using 9 components instead of 5.

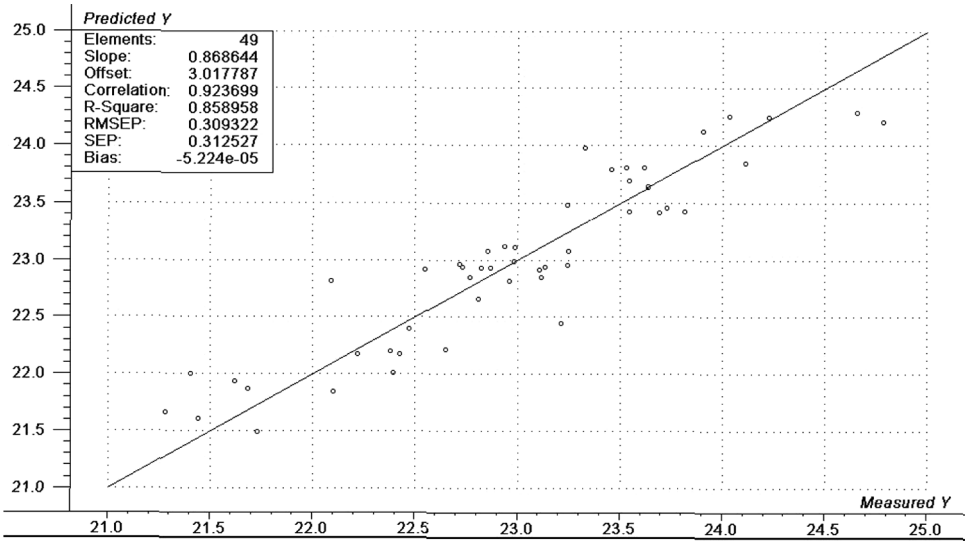

FIG. 6. Predicted versus measured values for the logarithmic form of the cake resistance $\alpha(ln(\alpha) = y)$.

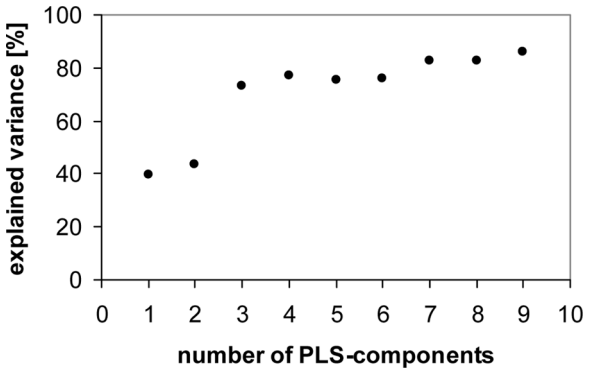

FIG. 7. Explained variances in the logarithm of the cake resistance ($ln(\alpha)$) versus the number of PLS –components included in the PLS-model.

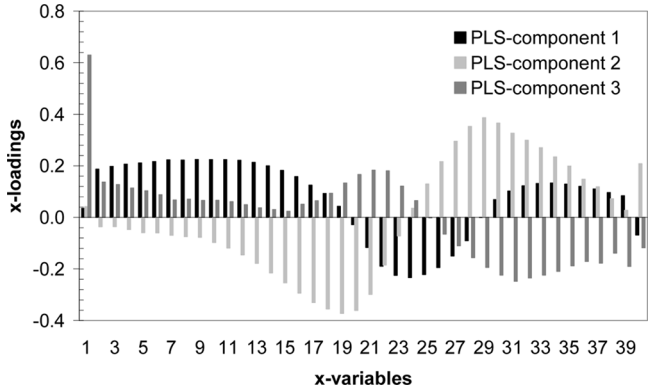

FIG. 9. Contribution of the x-variables to the first three latent variables (PLS-components) selected by PLS to explain the cake resistance values.

Figure 8 shows the regression coefficients, b_w, for prediction of the logarithm of the filter cake resistance ($ln(\alpha)$) from the variables presented in the experimental section. The regression coefficient for the first variable x_1 represents the filtration pressure difference (Δp). Regression coefficients 2–39 (for $x_2 - x_{39}$) characterize the 38 chord length distribution channels and the 40th regression coefficient (for x_{40}) describes the average cake porosity (ε).

The regression coefficients b_{w1}, $b_{w2}, \ldots, b_{wK}$ are used in the prediction model $\ln(\alpha) = y_w = b_{0w} + b_{w1}x_{1,w} + b_{w2}x_{2,w} + \ldots + b_{wK}x_{K,w}$ for the prediction of the y-variable ($ln(\alpha)$) in centred and scaled form. The elements in b_w, contrary to the respective elements in b used for prediction from the x-variables in their original forms, i.e. neither centred nor scaled, give the information about how much each x-variable influences the cake resistance ($ln(\alpha)$). Based on the criterion of $s(b_w) < 2|b_{wk}|$ (Jackknifing estimation) Fig. 8 shows that the only x-variables which influence the cake resistance significantly are x_1: the pressure difference and the number fractions of the chord length intervals x_{16}: $9.3 - 10.2\,\mu m$ x_{21}: $20.0 - 23.3\,\mu m$ x_{27}: $50.3 - 68.3\,\mu m$ and x_{30}: $79.7 - 92.9\,\mu m$. The variable x_{40}: the porosity of the filter cake, has no significant influence on the cake resistance according to the Jackknifing criterion. The contribution of the x-variables to the first three latent variables or PLS-components (equation the loadings of the x-variables, p_{ka}) is presented in Fig. 9. The loadings confirm the variation of x_1: the pressure difference, independent of the other variables and vice versa while x_{40}: the porosity of the filter cake correlates much with the chord length distribution. This could explain the lack of significance of the influence of porosity alone on the cake resistance.

Sensitivity Analysis

Sensitivity analysis of the obtained experimental data shows that both the applied pressure difference (Fig. 10) and the porosity (Fig. 11) influence the cake resistance significantly. The influence of the pressure difference (x_1), however, is more significant. The cake resistance increases with an increase in applied pressuredifference (x_1) and decreases with increasing porosity (x_{40}). The dependencies of the cake resistance on both the applied pressure difference and the porosity is in good agreement with basic

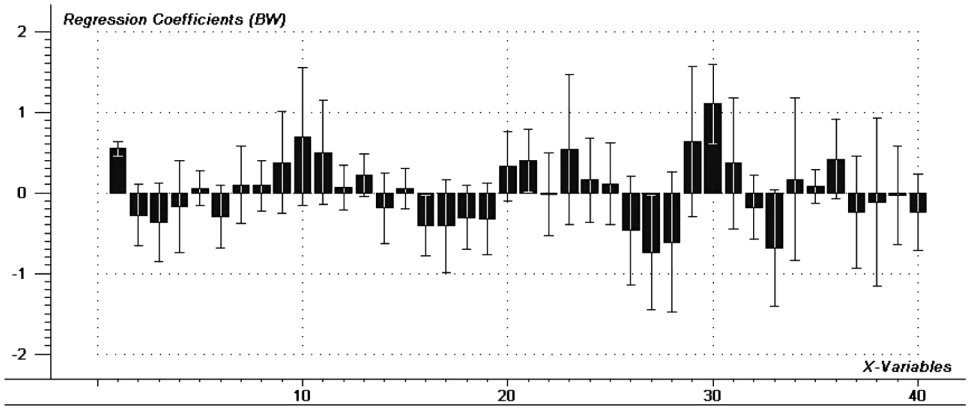

FIG. 8. The respective regression coefficients, b_w, for prediction of $ln(\alpha)$.

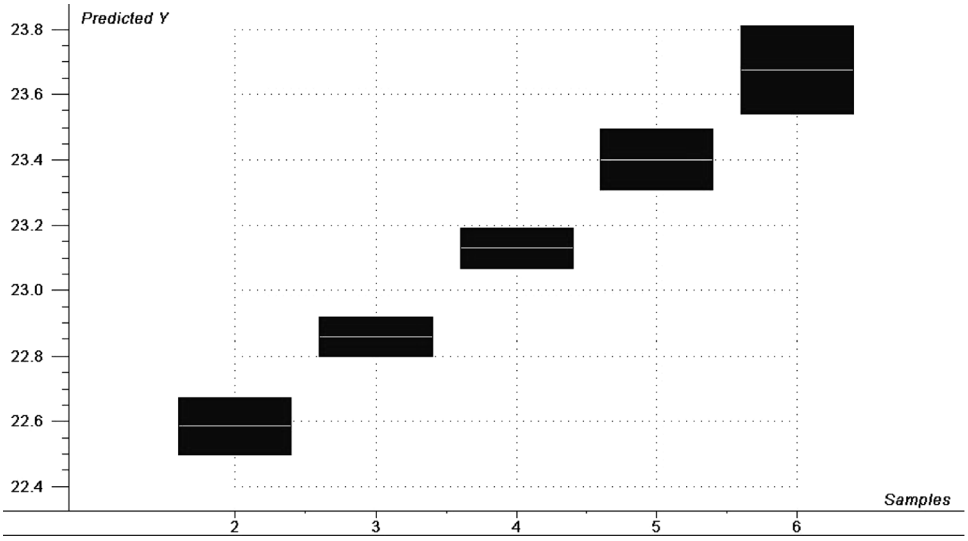

FIG. 10. Predicted variation in the logarithm of the cake resistance ($ln(\alpha)$) from a simulated variation in the pressure difference (x_1) with the other x-variables set constant and equal to their mean values.

filtration theory (see. Introduction). To examine the influence of the chord length distribution on ($ln(\alpha)$), the following simulation of X can be performed prior to the prediction (24):

$$\begin{aligned} \mathrm{X}_{\text{simulated}} &= \left(\bar{\mathrm{x}}_{\Delta\mathrm{p}} | \mathrm{X}_{\text{chord length distr, simulated}} | \bar{\mathrm{x}}_{\varepsilon}\right) \\ &= \left(\bar{\mathrm{x}}_{\Delta\mathrm{p}} | \mathrm{t}_{\text{simulated}}\ \mathrm{p}_{a,\ \text{from PLS of whole X}} | \bar{\mathrm{x}}_{\varepsilon}\right) \end{aligned}$$

for $a = 1, \ldots, A$, where A is the number of PLS-components for max explanation of $\mathrm{y} = \ln(\alpha)$. In this case $\mathrm{p}_a = (p_{2a} \ldots p_{ka} \ldots p_{K-1a})$ where A is the number of variables included in PLS.

In Figs. 12, 14, 16, and 18 the variations in the chord length distribution are simulated by varying one latent variable or combinations of several latent variables. In Figs. 13, 15, 17, and 19 variations in the cake resistance are predicted from the simulated variations in the chord length distributions presented in Figs. 12, 14, 16, and 18, respectively. The variation was simulated by optimizing the regression function constrained by the latent variables. The ranges of variation of all x_k were $\bar{x}_k \pm 1.5s(x_k)$ unless constrained by the latent variables.

The simulated chord length distributions based on variation in the first latent variable (Fig. 12) give a significant

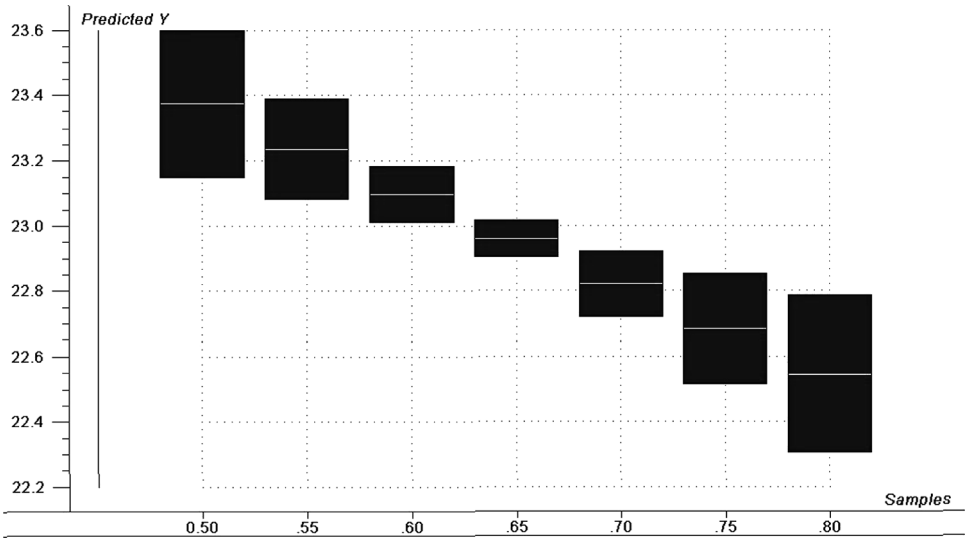

FIG. 11. Predicted variation in the logarithm of the cake resistance ($ln(\alpha) = y$) from a simulated variation in the porosity with the other x-variables set constant and equal to their mean values.

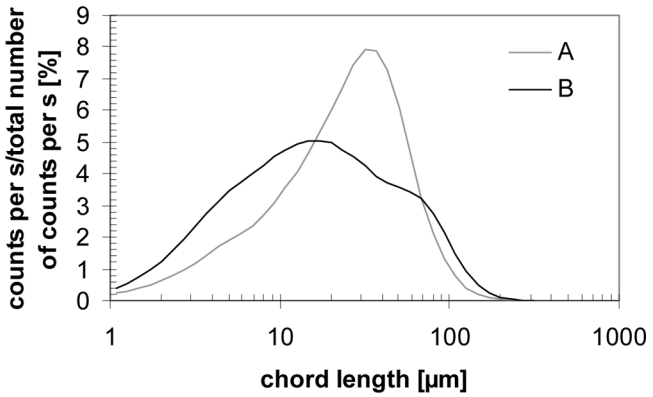

FIG. 12. Simulated variation in the chord length distribution by varying the first latent variable.

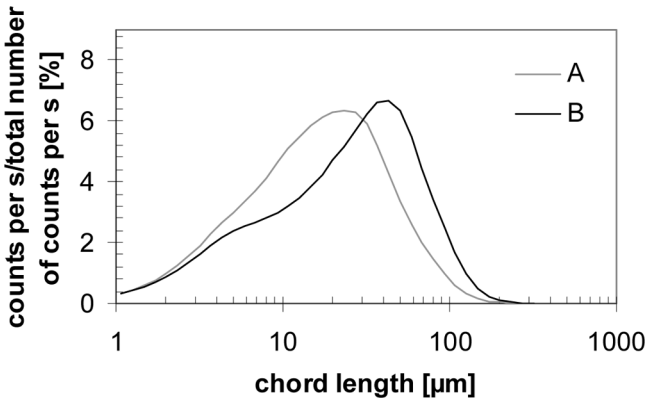

FIG. 14. Simulated variation in the chord length distribution by varying the second latent variable.

response in the resulting cake resistance (Fig. 13). The same is true for the simulation based on the second latent variable (Figs. 14 and 15). This is in accordance with Fig. 9 which shows relatively high loadings for the x-values that represent the chord length distribution. The response by variation in the third PLS-component is moderate both with respect to the simulated chord length distribution (Fig. 16) and the resulting cake resistance (Fig. 17), which can be explained by the fact that the third latent variable is dominated by the pressure difference.

The simulations of chord length distributions presented in Fig. 18 are based on an optimization of a combination of the first four latent variables in order to minimize and maximize the resulting cake resistance. The resulting maximum and minimum values of the cake resistance ($ln(\alpha)$) is presented in Fig. 19.

Sensitivity analysis and optimization performed on the basis of the experimental data leads to the conclusion that a broader chord length distribution with a larger percentage of smaller chord lengths coheres with a higher value for the average cake resistance (Fig. 19).

Cake Compressibility

The important role of the compression of the filter cake during filtration is illustrated by the significant regression coefficient (Fig. 8) and loading (Fig. 9) for the applied pressure difference during the filtration process. The fact that the cake resistance is mainly affected by the applied pressure difference with only minor dependence on the average porosity requires a closer look on the particle-particle and particle-liquid interactions within the cake. Wakeman and Tarleton (10) illustrate that the total applied pressure is partly converted into the solids compressible pressure acting on the particles within the cake, depending on the examined cake height. The solids compressible pressure in turn leads to a reduction in porosity of compressible cakes and hence more resistant cakes. Grace (28) presents filtration results for 17 tested materials showing that the specific cake resistance increases and the porosity decreases by increasing the compressive pressure exerted on the particles from 0.07 bar to 186 bar. Tiller (29) shows the results of experimentally determined values for the porosity of materials

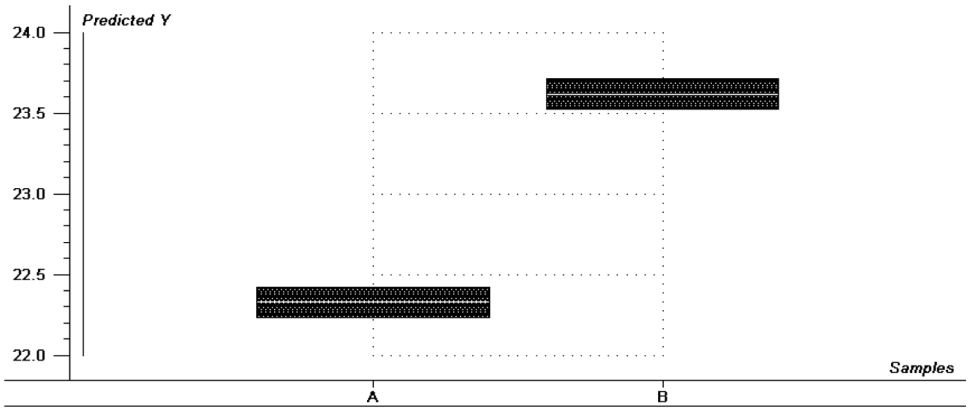

FIG. 13. Variation in the logarithm of the cake resistance ($ln(\alpha) = y$) predicted from the chord length distributions presented in Figure 12. The other variables are kept constant and equal to their mean values.

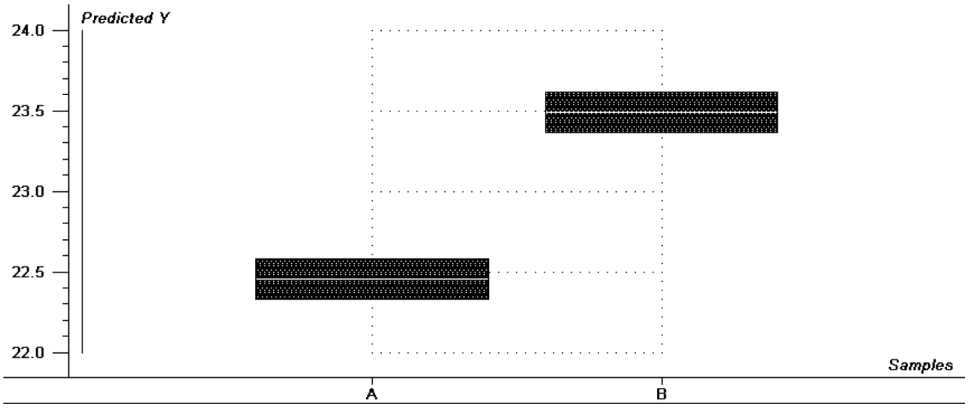

FIG. 15. Variation in the logarithm of the cake resistance ($ln(\alpha) = y$) predicted from the chord length distributions presented in Figure 14. The other variables are kept constant and equal to their mean values.

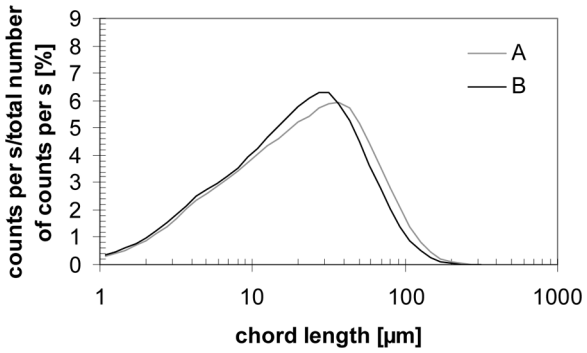

FIG. 16. Simulated variation in the chord length distribution by varying the third latent variable.

such as kaolin, calcium carbonate and asbestos, in dependence of the applied solids compressible pressure of up to 7 bar. From the obtained results he concludes that the porosity can be satisfactorily related to the pressure by a power function. Both empirical models (13) and mechanistic models (30–34) have been used in the attempt to capture the characteristics of compressible cakes. According to Wakeman and Tarleton (10) the solids compressible pressure increases non-linearly from the cake surface to the filter cloth as the hydraulic pressure is transmitted by the liquid to the particles by friction and then from particle to particle. As a consequence of the increase in the solids compressible pressure towards the filter cloth, Zogg (35,36) illustrates that compressible filter cakes display an incompressible layer at the cake surface, but are compressible to a higher extent as the distance from the cake surface increases. These findings make it possible to explain why the cake resistance significantly depends (Fig. 5 and 6) on the applied pressure difference and why the measured average porosity is far less significant. It is proposed that the compression of layers close to the filter medium leads to a low local porosity while the average porosity is nearly unchanged. As a result, cake resistance values are found to increase strongly with the applied pressure difference. The dependency can be

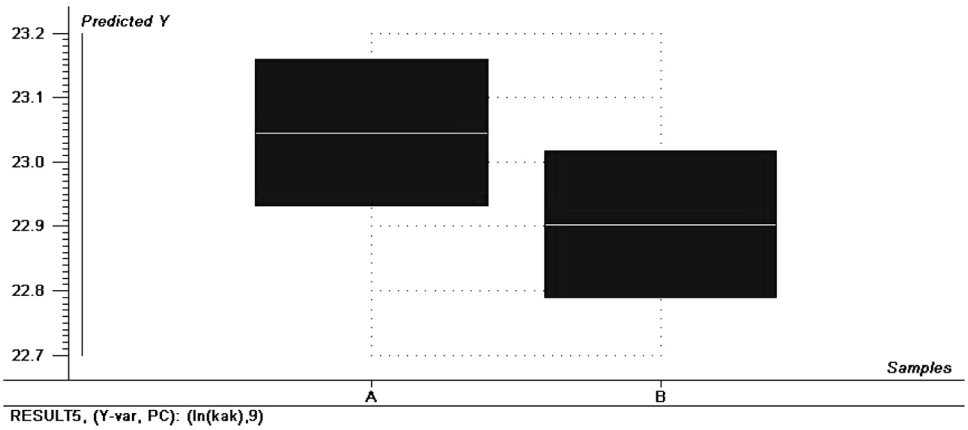

FIG. 17. Variation in the logarithm of the cake resistance ($ln(\alpha) = y$) predicted from the chord length distributions presented in Figure 16. The other variables are kept constant and equal to their mean values.

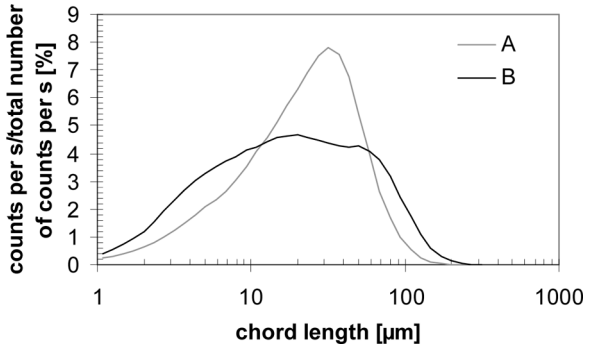

FIG. 18. Simulated variation in the chord length distribution by varying the optimal combination of the four first latent variables, $(n_1\ n_2\ n_3\ n_4) = (0.59\ 0.23\ 0.13\ 0.05)$.

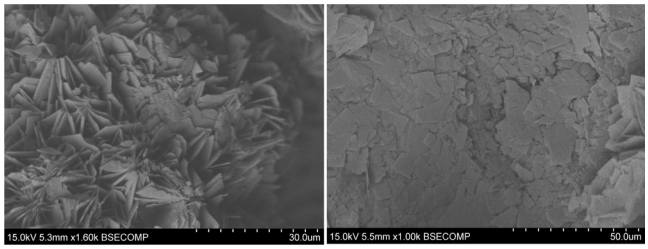

(a) (b)

FIG. 20. Crystals produced at 60°C and S = 6 taken from the filter cake after filtration at 2 bar: (a) shows the damaged surface of the particles and (b) shows plate-like crystals that have arisen during the crystallization and filtration process.

expressed as a power function (10) which explains why a logarithmic transformation of the measured cake resistance values yielded a higher quality model (Fig. 6). The strong local compression of the filter cake might originate by different mechanisms. The observed spherulites are susceptible to disintegration by breakage or ageing during the filtration process. Then, smaller plate-like crystals arising during crystallization and filtration might migrate into the deeper laying pores of the filter cake (32,34). This is supported by the sensitivity analysis which shows that broader chord length distributions due to smaller particles give rise to higher cake resistance values (Figs. 12–15 and 18–19). Finally, also the rearrangement of the particles composing the cake can lead to a compaction of the cake. The compressible behavior of the investigated crystals is confirmed by the pictures depicted in Fig. 20 where the surface of the crystalline material is shown to be damaged (Fig. 20a), and by the plate-like particles in Fig. 20b originating from crystallization and filtration.

SUMMARY AND CONCLUSIONS

Partial least squares regression and sensitivity analysis were used to study the influence of the measured chord length distribution of different crystal suspensions, the effect of the average cake porosity and the applied filtration pressure difference on the average cake resistance of polycrystalline particles of an aromatic amine. Analysis of the results has disclosed that wider chord length distributions as well as lower values of the measured average porosity lead to higher values for the average cake resistance. The fact that lower average porosity leads to more resistant cakes is in accordance with general filtration theory, partly as a consequence of a wider particle size distribution. However, it has been shown that the applied pressure difference itself plays a more significant role in explaining the measured average cake resistance values than the measured average porosity. The fact that an increase in the applied pressure difference has a more significant influence on the increase in the average cake resistance than could be expected from the average porosity can be explained by cake compression of the filter cake occurring predominantly

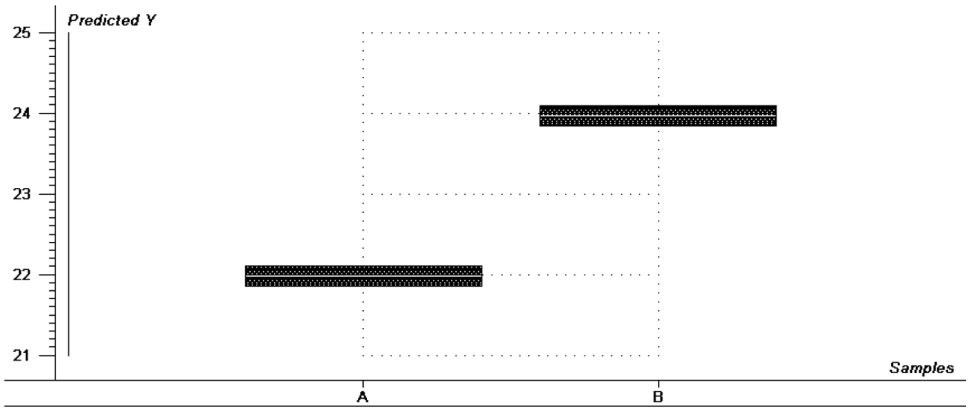

FIG. 19. Variation in the logarithm of the cake resistance $(ln(\alpha) = y)$ predicted from the chord length distributions presented in Figure 18. The other variables are kept constant and equal to their mean values.

close to the filter cloth. Cake compression above the filter cloth leads to low local porosity which has previously been reported for highly compressible cakes (37). Cake compression is proposed to be effected by disintegration of unstable polycrystalline particles forming the cake and by invasion of smaller plate-like particles into deeper lying pores of the filter cake. Hence, owing to high filter cake resistances in the aromatic amine system associated with the formation of unstable polycrystalline particles, such particle morphologies should, if possible, be avoided in industrial crystallization processes.

ACKNOWLEDGEMENTS

The authors thank the Norwegian Research Council, GE Healthcare, StatoilHydro, Dyno Nobel, Norcem, and Hydro Aluminium for their financial support.

NOMENCLATURE

a	number of latent variables
A	filter area, maximum number of latent variables, number of PLS components for max explanation of y, variable
b	regression coefficient
b_w	weighted regression coefficient
c	weight fraction of dissolved substance [g/g solution], variable
c^*	solubility weight fraction [g/g solution]
E	residual in X
F	residual in Y
h	cake height
i	observation number, variable
I_{pr}	number of validation objects
k	variable number
K	number of variables included in the PLS model
m_s	mass of dry solids
n	optimal value for latent variables
p, P	x variable loading
Q	y variable loading
s	standard deviation
s_{mfs}	mass fraction of solids in the feed [g/g suspension]
S	supersaturation ratio
t	filtration time
T	temperature
T, t	factor score in X
U	factor score in Y
V	filtrate volume
x_{ecs}	effective concentration of solids [g/ml filtrate], predictor variable
x	predictor variable
$\bar{x}$	mean value of the predictor variable
X	matrix of predictor variables
y	observed variable
$\hat{y}$	predicted value for the response (predicted variable)
Y	matrix of predicted variables
α	average specific cake resistance [m/kg]
β	filter medium resistance [1/m]
Δp	pressure difference
ϵ	average cake porosity
η	dynamic viscosity
ρ_l	filtrate density
ρ_s	density of solids
ATR	Attenuated Total Reflectance
FBRM	Focused Beam Reflectance Measurement
IR	Infrared
PLS	Partial Least Squares
SEM	Scanning Electron Microscopy

REFERENCES

1. Mullin, J.W. (2001) *Crystallization*, 4th Ed.; Elsevier Butterworth-Heinemann: Oxford, UK.
2. Wakeman, R. (2007) The influence of particle properties on filtration. *Separation & Purification Technology*, 58: 234.
3. Holdich, R. (2002) *Fundamentals of Particle Technology*; Midland Information Technology and Publishing: Shepshed, Leicestershire, UK.
4. Sorrentino, J.A.; Anlauf, H. (2004) Prediction of filter-cake properties from particle collective characteristics. *Fluid/Particle Separation Journal*, 16: 135.
5. Tiller, F.M. (1975) What the filter man should know about theory. *Filtration & Separation*, 12: 386.
6. Carman, P.C. (1937) Fluid flow through granular beds. *Transactions of the Institution of Chemical Engineers*, 15: 150.
7. Carman, P.C. (1938) Determination of the specific surface of powders. Part I. *Journal of the Society of Chemical Industry*, 57: 225.
8. Carman, P.C. (1939) Determination of the specific surface of powders. Part II. *Journal of the Society of Chemical Industry*, 58: 1.
9. Kozeny, J. (1927) Über kapillare Leitung des Wassers im Boden. *Sitzungsberichte der Akademie der Wissenschaften in Wien*, 136: 270.
10. Wakeman, R.; Tarleton, S. (2005) *Solid Liquid Separation, Principles of Industrial Filtration*, 1st Ed.; Elsevier: Oxford, GB, UK.
11. Tiller, F.M.; Crump, J.R. (1977) Solid-liquid separation: An overview. *Chemical Engineering Progress*, 73: 65.
12. Rushton, A.; Hosseini, M.; Hassan, I. (1978) The effects of velocity and concentration on filter cake resistance, pp. 78–91, Proc. Symp. on Solid-Liquid Separation Practice, Leeds, UK, Yorkshire Branch of the I. Chem. E., 27th-29th March 1978.
13. Häkkinen, A.; Pöllänen, K.; Reinikainen, S.-P.; Louhi-Kultanen, M.; Nyström, L. (2008) Prediction of filtration characteristics by multivariate data analysis. *Filtration*, 8: 144.
14. Liotta, V.; Sabesan, V. (2004) Monitoring and feedback control supersaturation using ATR FTIR to produce an active pharmaceutical ingredient of a desired crystal size. *Organic Process Research & Development*, 8: 488.
15. Esbensen, K.H. (2002) *Multivariate Data Analysis in Practice: An Introduction to Multivariate Data Analysis and Experimental Design*, 5th Ed.; Camo Process AS: Oslo, Norway.
16. Togkalidou, T.; Braatz, R.; Johnson, B.K.; Davison, O.; Andrews, A. (2001) Experimental design and inferential modeling in pharmaceutical crystallization. *AIChE Journal*, 47: 160.
17. Høskuldsson, A. (1996) *Prediction Methods in Science and Technology*, vol. 1; Thor Publishing: Copenhagen, Denmark, p. 266.

18. Beck, R., Malthe-Sørenssen, D., Andreassen, J.P. (2009) Polycrystalline growth in precipitation of an aromatic amine derivative and L-Glutamic Acid. *Journal of Crystal Growth*, 311: 320.
19. Ruf, A., Worlitschek, J., Mazzotti, M. (2000) Modeling and experimental analysis of PSD measurements through FBRM. *Particle & Particle Systems Characterization*, 17: 167.
20. Mota, M.; Teixeira, J.A.; Bowen, W.R.; Yelshin, A. (2003) Interference of coarse and fine particles of different shape in mixed porous beds and filter cakes. *Minerals Engineering*, 16: 135.
21. Svarovsky, L. (2000) *Solid-Liquid Separation*, 4th Ed.; Butterworth-Heinemann: Oxford, GB, UK.
22. Martens, H.; Martens, M. (2000) Modified Jack-knife estimation of parameter uncertainty in bilinear modeling by partial least squares regression (PLSR). *Food quality and preference*, 11: 5.
23. Svinning, K.; Datu, K.A. (2003) Prediction of microstructure and properties of Portland cement from production conditions in cement mill: Part II. Prediction and sensitivity analysis, 11th International Congress on the Chemistry of Cement, Durban, South Africa.
24. Svinning, K. (2006) Design and manufacture of Portland cement – application of sensitivity analysis in exploration and optimisation: Part I: Exploration. *Chemometrics and Intelligent Laboratory Systems*, 84: 177.
25. Svinning, K.; Ingerøyen, Ø.; Dalsveen, K. (2000) Optimization of a response variable y constrained by principal directions in variations in the observation X-matrix. *J. Chemometrics*, 14: 699.
26. Svinning, K.; Høskuldsson, A. (2006) Design and manufacture of Portland cement – application of sensitivity analysis in exploration and optimization: Part II. Optimisation. *Chemometrics and Intelligent Laboratory Systems*, 84: 188.
27. Nelder, J.A.; Mead, R. (1965) A simplex method for function minimization. *Comput. J.*, 7: 308.
28. Grace, H.P. (1953) Resistance and compressibility of filter cakes, Part I. *Chemical Engineering Progress*, 49: 303.
29. Tiller, F.M. (1953) The role of porosity in filtration, numerical methods for constant rate and constant pressure filtration based on Kozeny's Law. *Chemical Engineering Progress*, 49: 467.
30. Holdich, R.G. (1990) Solids concentration and pressure profiles during compressible cake filtration. *Chemical Engineering Communications*, 91: 255.
31. Abboud, N.M., Corapcioglu, M.Y. (1993) Modeling of compressible cake filtration. *Journal of Colloid and Interface Science*, 160: 304.
32. Lu, W.-M.; Huang, Y.-P.; Hwang, K.-J. (1998) Methods to determine the relationship between cake properties and solid compressive pressure. *Separation & Purification Technology*, 13: 9.
33. Tien, C.; Bai, R.; Ramarao, B.V. (1997) Analysis of cake growth in cake filtration: Effect of fine particle retention. *AICHE J.*, 43: 33.
34. Civan, F. (1998) Practical model for compressive cake filtration including fine particle invasion. *AIChE Journal*, 44: 2388.
35. Zogg, M. (1979) Filtration mit kompressiblem Kuchen. *Swiss Chem*, 1: 27.
36. Zogg, M. (1980) Experimentelle Bestimmung der Filtrationseigenschaften kompressibler Filterkuchen. *Swiss Chem*, 2: 43.
37. Li, W., Tiller, F.M. (2004) Characterizing the super-compactibility of wastewater filter cakes. *Fluid/Particle Separation Journal*, 16: 27.